



IJRASET

International Journal For Research in
Applied Science and Engineering Technology



INTERNATIONAL JOURNAL FOR RESEARCH

IN APPLIED SCIENCE & ENGINEERING TECHNOLOGY

Volume: 10 Issue: VI Month of publication: June 2022

DOI: <https://doi.org/10.22214/ijraset.2022.44163>

www.ijraset.com

Call:  08813907089

E-mail ID: ijraset@gmail.com

Microgrid Protection and Fault Analysis

Sangeeta Modi¹, Dr. P Usha²

¹Research Scholar, Visvesvaraya Technological University, Belagavi

²Dayananda Sagar College of Engineering, Bangalore

Abstract: *Microgrid is an active distribution network. It can be operated in various modes of operation such as grid connected mode and islanded mode. Integration of distributed generation can provide solution to the power crisis over the globe. But there are various challenges involved in integration of microgrids to the conventional grid. One of the major challenges in the implementation of microgrid is protection of the microgrid. Very little attention has been paid towards microgrids protection which is highly required to ensure safety and reliability of the overall system. In this paper, a hybrid microgrid system has been analysed on the DC side against various types of faults such as Pole to pole fault and pole to ground fault. Results reveal that pole-to-pole fault is more severe than pole to ground fault. Further, a memory based current algorithm has been applied to detect the fault in the microgrid and it was observed that this algorithm is suitable for the detection of the fault in the microgrid. The effectiveness of the controller based on current algorithm has been tested in MATLAB environment.*

Keywords: *Microgrids, Fault Analysis, Protection of Microgrid, Pole to pole fault, pole to ground fault*

I. INTRODUCTION

Microgrid is an active distribution network. It can be operated in various modes of operation such as grid connected mode and islanded mode. Microgrid is a group of distributed generators located at customer place or it may be connected to the distribution system at a dedicated place. Renewable energy sources such as solar wind have observed rapid increase in usage in the microgrid due to sustainable energy goals. There are various types of microgrids based on the load served such as AC microgrid, DC microgrid and hybrid microgrid. In an AC microgrid various types of distributed generators loads and storage devices are connected to a common AC bus whereas in dc microgrids distributed energy resources, loads and energy storage devices (if any) are connected to a common DC bus.

Integration of distributed generation can provide solution to the power crisis over the globe. But there are various challenges involved in integration of microgrids to the conventional grid. One of the major challenges in the implementation of microgrid is protection of the microgrid. The difference in short circuit current in grid connected mode and islanded mode is the main reason behind this protection challenge. Microgrids deal with bidirectional flow of power which leads to blinding of protection. Integration of various distributed generators changes the fault current Which leads to malfunctioning of the connected protective gears such as setting of the relays connected at various points in the microgrid.

To provide good quality and reliable supply to the customer is the main goal of a microgrid. So, it is highly important to analyse the microgrids for various fault conditions. Conventional methods of protection are not suitable for the protection of the microgrid because of the various reasons mentioned above such as bidirectional flow of power and blinding etc.

The cluster of various distributed generators, storage devices, loads and power electronic interfaces in between makes microgrid different in terms of responding to the fault current in different way. Depending on the various types of configurations of the microgrid, Fault current may vary. So, coordination of the control gears is very much required. For this purpose, we need to analyse the system behaviour properly against various types of faults. Microgrid configuration plays very important role in deciding the settings of the protective devices. Depending upon the configuration selected fault current may vary in the various devices integrated in the system [1-3].

Protection part has been challenging for a dc system as compared to traditional ac distribution systems [5]. In reference [6] Grounding system is well explained, and differential protection algorithm has been applied. For fault location identification the traveling waves concept is applied which is caused by a fault. This approach has been modified for ac fault protection as well [7] The comparison between two arrival times along with the wave propagation velocity can identify the fault location.

One of the important requirements in microgrid protection is very fast real time communication channel in between the protective devices and the master controller unit to ensure security and reliability. Detection and location of fault can be found out with the help of these communication channels based on most sensible standards such as IEC 61850[3-4].

In [8] adaptive protection scheme is presented which monitors the microgrid continuously and updates relay fault current immediately according to the conditions in the system, but this scheme is not capable of finding the shortest path of isolation.[9].

The central controller presented involves the multiple features for proper coordination of distributed energy resources to serve the critical and non-critical loads. Initiation of protection techniques at the time of fault occurrence at the grid end or in microgrid ensures stability and reliability in the system.

In this [10] paper Microgrid components such as PV array, Boost converter and Inverter are modelled using mathematical equations in both Grid-Connected Mode and Islanded Mode of Operation.

In centralized protection, Microgrid Management System can be used to check or monitor the state of the microgrid and to set rating of the respective protection equipment. The communication of protective devices is based on standards IEC61850.

It is always advisable to divide the complete microgrid network into number of zones or sections. Point of common coupling (PCC) zone could be the main zone where high-speed circuit breakers (CBs) or smart switches (SS) are required depending on the type of the microgrid. Another zone could be the feeder protection zone where miniature CB's with suitable relays can be connected. Third zone could be the service zone near customer where suitable CB's or smart switches can be connected to appropriate devices for the detection of the fault. Fourth zone could be the zone in which DGs are connected.

In this work DC section of the hybrid microgrid has been analysed for various types of faults such as pole to pole fault and pole to ground faults. While designing any protection scheme for the microgrid system, fault analysis is required in detail. In this paper pole to pole and pole to ground fault analysis has been carried out on the selected microgrid at zone 1 which is near solar panels. Other zones are marked as zone 2 (near wind), zone 3(near Battery) and so on as shown in figure (2).

II. SYSTEM UNDER CONSIDERATION

Figure 1 shows the block diagram of the system under consideration. DC part of the system consists of PV source, wind power source, battery, and a DC load. There is a large development in ac distribution and transmission system protection technology because it is simple and easy to control whereas very little attention has been paid to the DC microgrid protection.

The protection of microgrid is possible with the help of various parameters like samples of current, voltage, angles, as well as some local variables such as rms current, rms voltage, voltage THD (Total Harmonic Distortion), current THD and symmetrical components of current and voltage.

A. Block Diagram of the System under Consideration

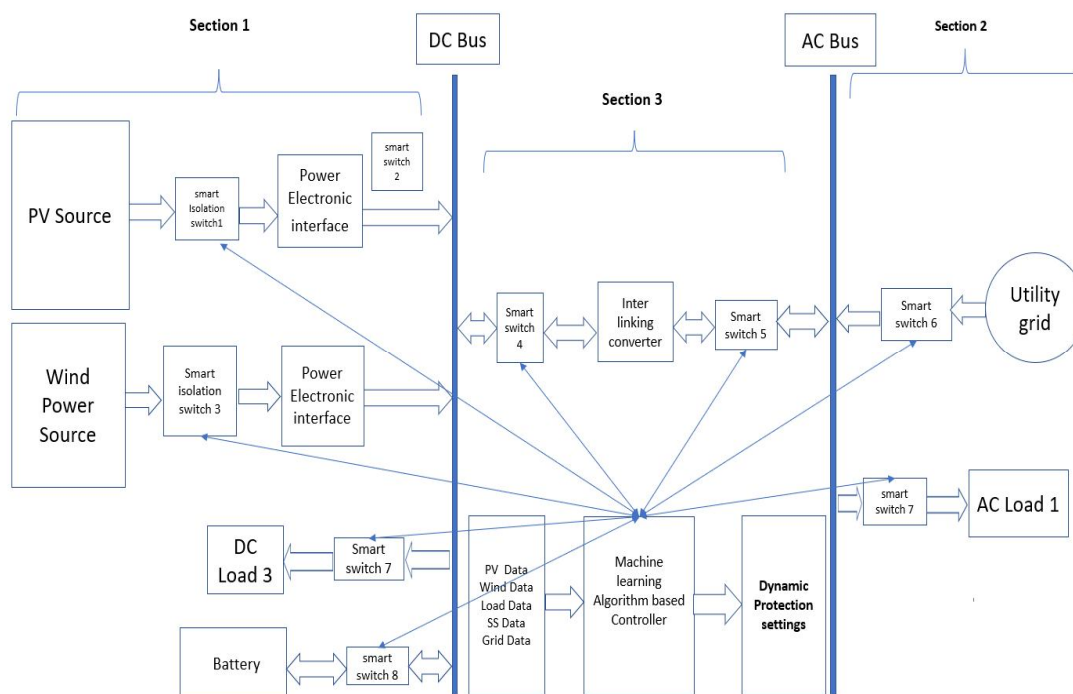


Figure 1

Figure (1) shows the block diagram of the system under consideration in this system utility grid of 3 phase, 25 Kw, 50 Hz is connected to a hybrid microgrid To reduce the burden. Hybrid microgrid consisted of solar panel, wind power source, battery and various power electronics interfaces. Voltage at point of common coupling is 500 V at DC bus , power supplied by solar is 50 kW. Wind power source can supply 50 kW . Battery (30kW , 500 V) is connected for the emergency conditions when there is no power available from PV source and wind power source then battery will share the power to the Load and utility grid depending on the mode of operation considered. AC load of 100 kW is connected to the AC bus.

B. Block Diagram of the System under Consideration under fault Condition at zone 1 (Near Solar Panel)

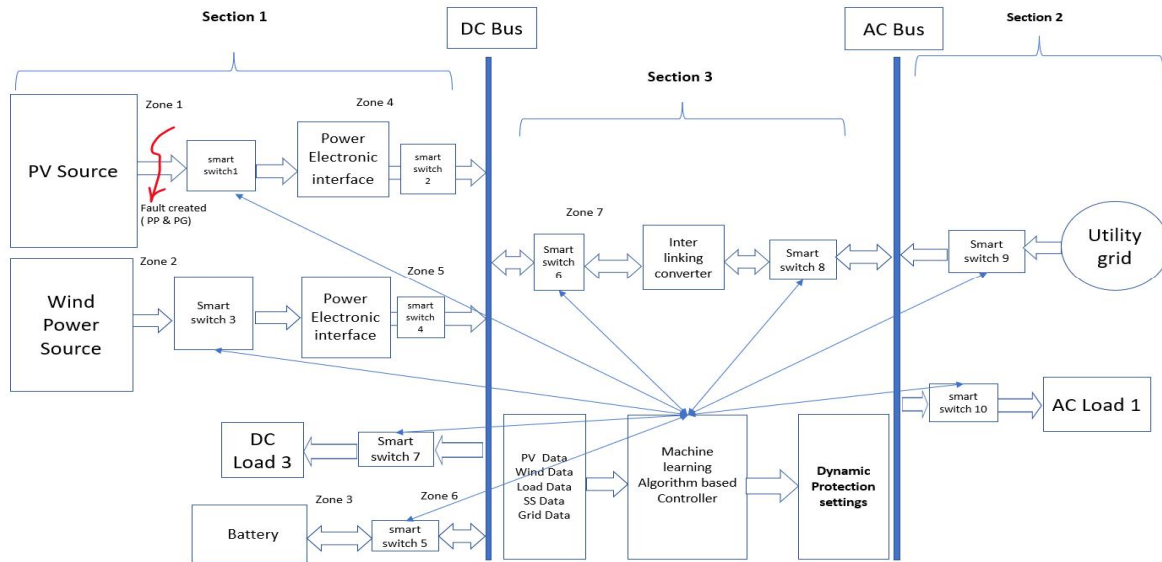


Figure 2

Based on the status of the microgrid received through monitoring devices, the protecting devices make comparison between the measured parameter and the operating curves set then provides trip signal. In this work, samples of current are taken and compared with the previous sample to check the error and to initiate the operation of the protective gears connected to the system to isolating the affected zone quickly.

III.SIMULATION RESULTS AND CONCLUSION

A. Simulation Results and Analysis – Under Normal condition (without fault)

Analysis of the system under Normal and fault condition

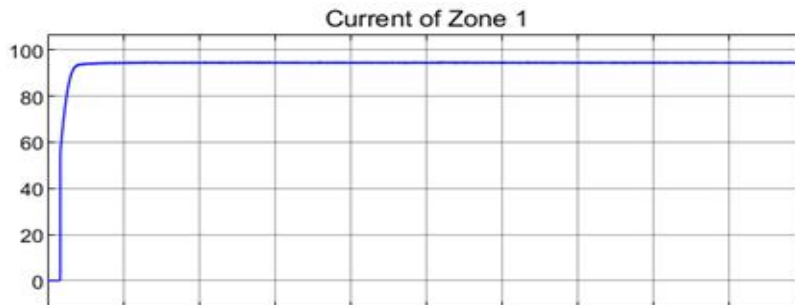


Figure 3

Figure 3 shows the current flowing through Zone 1 under normal conditions. the x-axis represents the time of simulation while the y-axis represents the current readings of the Zone in Amperes. The value of current takes about 0.03 seconds of simulation time to reach steady state value, of about 94-94A. Under normal conditions, where no disturbance or sudden change occurs in the system under consideration, the steady state value of current is maintained.

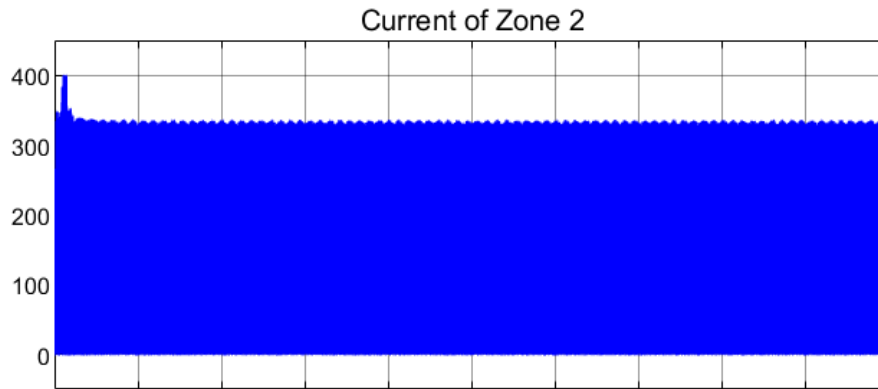


Figure 4

The current of Zone 2 under normal conditions is graphed in Figure 4. Zone 2 is defined as the area after the wind turbine system and before the wind system breaker. The x-axis represents the time of simulation in Simulink while y-axis represents the reading of the current measurement unit in Zone 2. In Figure 4, there is a momentary spike to about 400A observed in the current reading after which it settled down at 340 A.

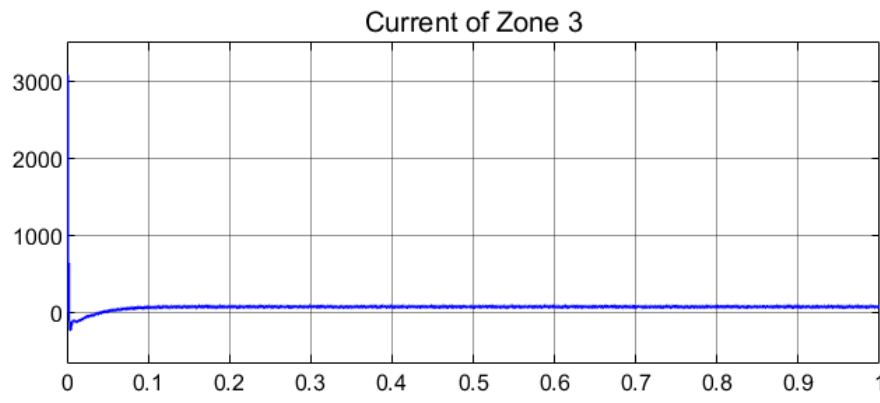


Figure 5

The current readings of Zone 3 under normal conditions are graphically displayed in Figure 5. The observed values are indicative of an initial momentary spike to almost 3000A. The following values indicate a dip and a stabilization of readings to around 100A by 0.1 seconds of simulation time.

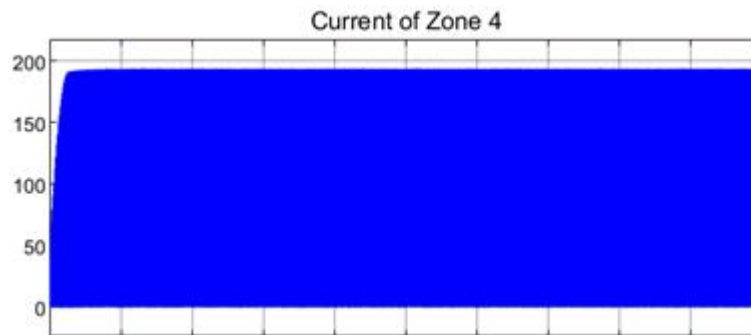


Figure 6

Figure 6 represents the current readings of Zone 4 under normal conditions where x-axis represents the time of simulation and y-axis represents the current readings of the line (in Amperes) under normal conditions. Steady state is reached at around 190A at a simulation time of 0.4 seconds.

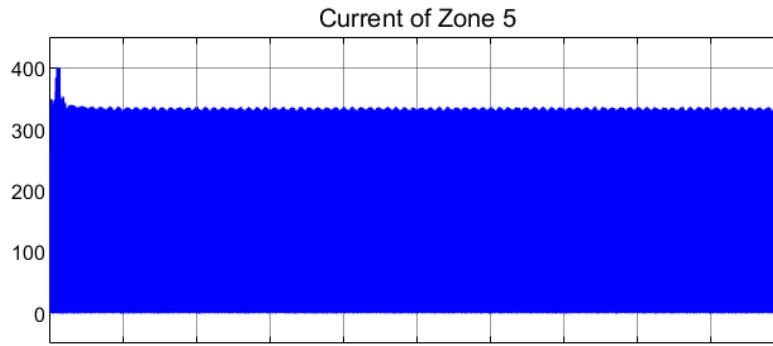


Figure 7

The current readings under normal conditions (in Amperes) of Zone 5 is presented in Figure 7. There is a momentary spike of 400A which is observed for a few cycles, after which a steady state value in transients between 0A and 310A is observed.

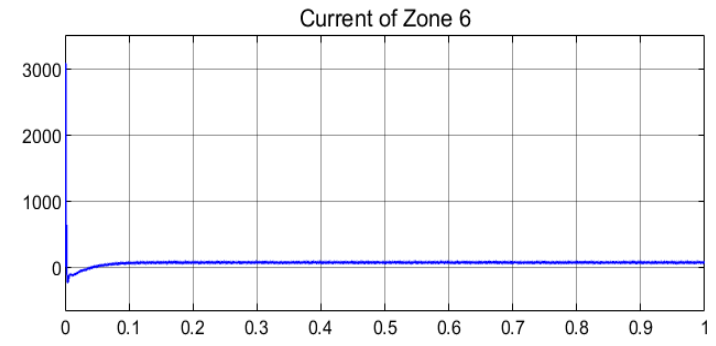


Figure 8

Figure 8 represents the current through Zone 6 under simulation of normal conditions, i.e. where no fault or disturbance affects the system under consideration. There is an initial spike observed to about 3000A after which the current reduces drastically. This is followed by a reach to steady state value by the current readings at around 100A.

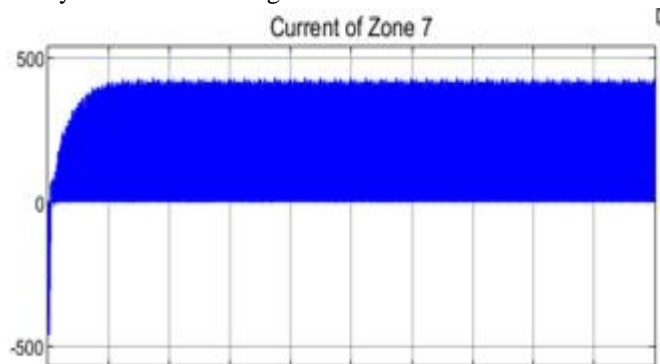


Figure 9

The current readings of Zone 7 (in Amperes) under normal conditions is Figure 9, where x-axis represents the time of simulation and y-axis represents the current readings of the measurement unit in Zone 7. An initial drop to almost -500 A is observed for a few cycles after which the value stabilizes to transients between 0A and about 400A, thus reaching steady state by around a simulation time of 0.07A.

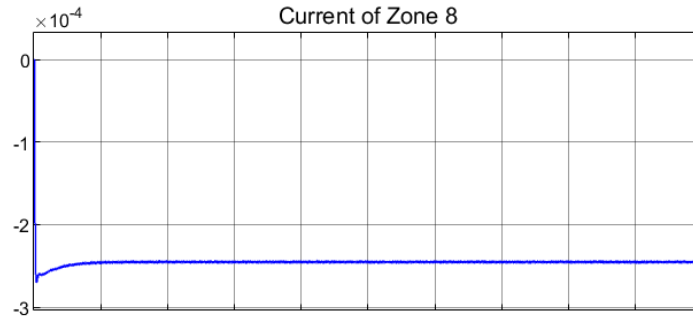


Figure 10

Figure 10 displays the current readings, in Amperes, in Zone 8 under normal conditions. The value of current drops to -2.6×10^{-4} A and reaches a steady state value of -2.5×10^{-4} A at a simulation time of around 0.05 seconds.

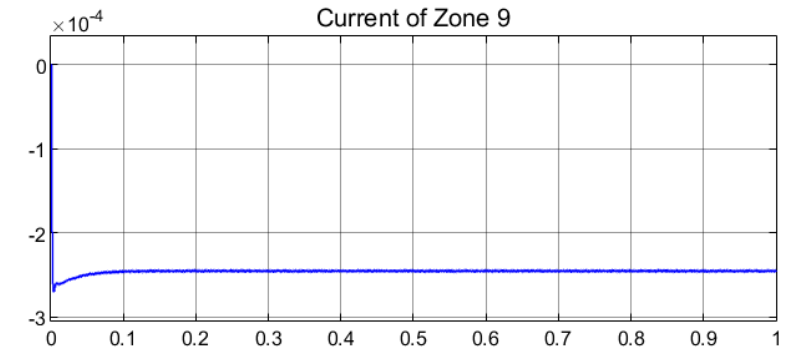


Figure 11

The current of Zone 9 under normal conditions, where x-axis represents time of simulation in Simulink and y-axis represents the current reading in A, is displayed in Figure 11. The value of current drops to -2.6×10^{-4} A and reaches a steady state value of -2.5×10^{-4} A at a simulation time of around 0.05 seconds.

B. Simulation Results and Analysis – Under Pole to pole fault condition



Figure 12

When a pole-to-pole fault is simulated at Zone 1, the current change is observed and displayed in Figure 21. While the x-axis represents the simulation time in seconds, y-axis represents the current of Zone 1 in Amperes. The fault is created in about 1.000 second of simulation time and it is observed that the current drops from a steady state value of around 95A to a value of around -2600A and stabilizes there.

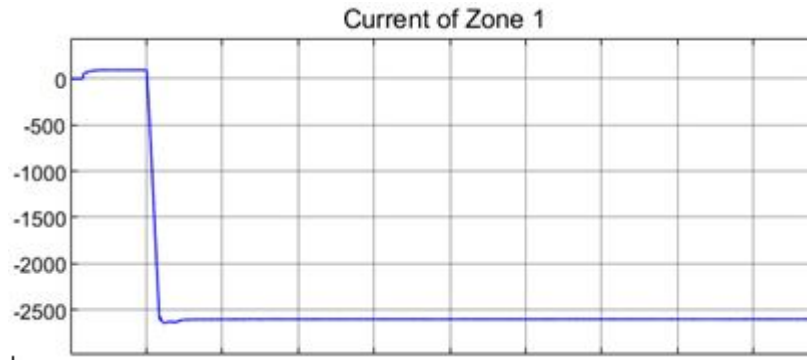


Figure 13

When a pole-to-pole fault is created at Zone 1, Figure 13 showing the current measurements of Zone 2 shows that there is a decrease in current from around transients between 0A and 320A to transients between 0A and 280A.

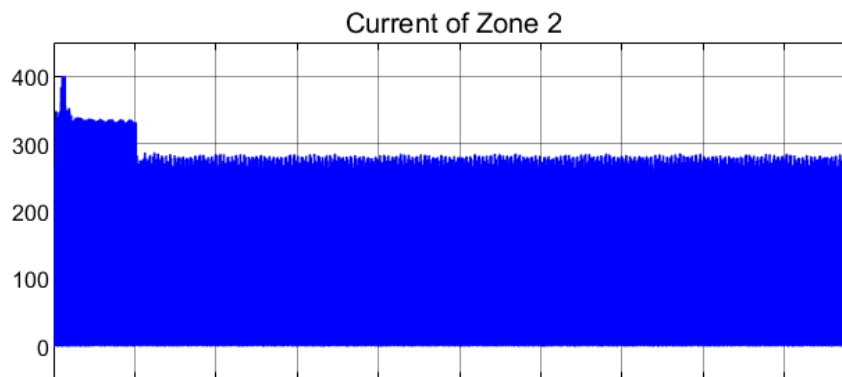


Figure 14

Figure 14 shows the current observations in Zone 3 when a p-p fault is created in Zone 1. When a fault is created, the value of current shows a drastic, immediate increase from a steady state value of 100A to 1900A. This value decreases to around 1600A and stabilizes with transients.

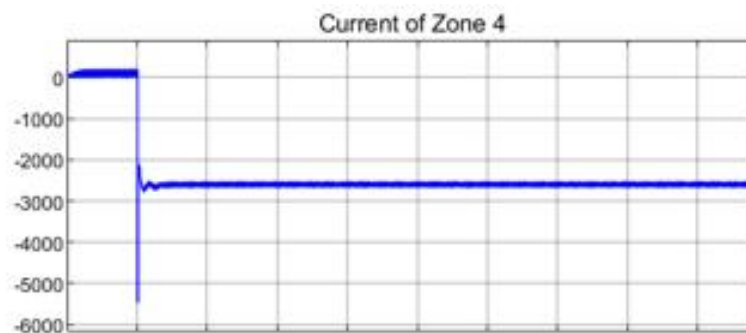


Figure 15

When a p-p fault is created a Zone 1, Figure 15 displays the current measurements in Zone 4, when the fault is created at a simulation time of 1.00. When the fault is created, a momentary decrease to -5500A from steady state value is observed followed by stabilization with transients around -2500A.

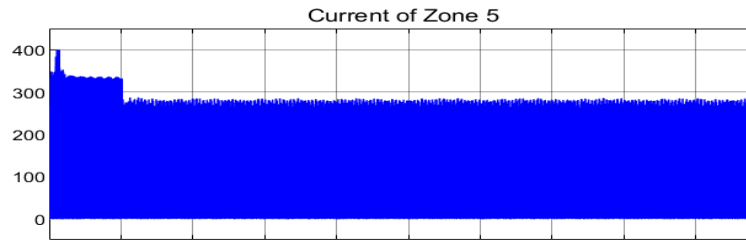


Figure 16

When a p-p fault is created at Zone 1, Figure 16 shows Zone 5’s current measurement with x-axis representing the simulation time and y-axis representing the output of the current measurement device. Once the fault has occurred, decrease in the observed transients from 0A to 325A to stabilization between 0A to 280A is observed.

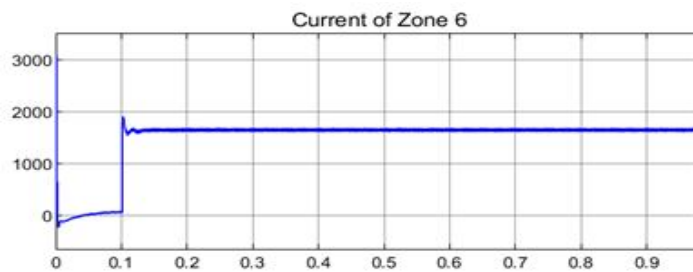


Figure 17

Figure 17 shows the measurement of current at Zone 6 when a p-p fault occurs at Zone 1. When the fault has occurred at a simulation time of 1.000, a sudden spike in current is observed followed by a stabilization with transients around 1600A.

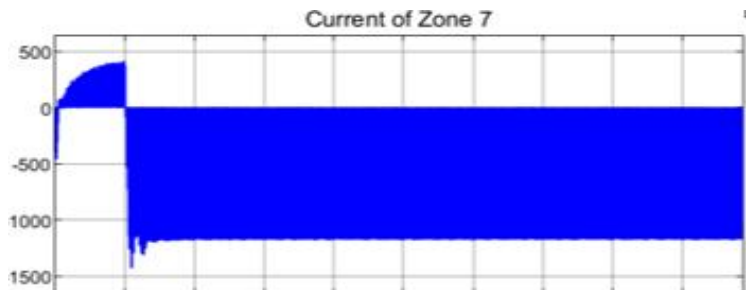


Figure 18

Figure 18 represents the current through Zone 7 when a p-p fault is created at Zone 1 at a simulation time of 1.000. The observed current shows a decrease to -1450A from steady state value and a slight increase to stabilization at -1100A.

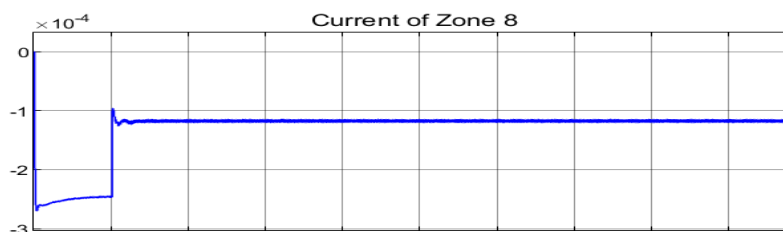


Figure 19

Figure 19 represents the current through Zone 8 when a p-p fault is created at Zone 1 with x-axis representing the time and the y-axis representing the current of the Zone in Amperes. The current value increases from steady state value to a peak at $-1 \times 10^{-4}A$ to stabilization with transients around $-1.15 \times 10^{-4}A$

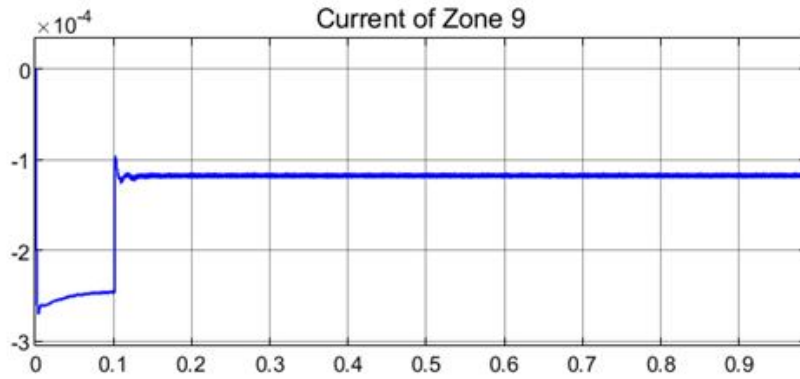


Figure 20

Figure 20 represents the current measurement in Zone 9 after a fault has been created at a simulation time of 1.000 in Zone 1. The current value increases from steady state value to a peak at $-1 \times 10^{-4} \text{A}$ to stabilization with transients around $-1.15 \times 10^{-4} \text{A}$.

C. Comparative Analysis of PP and PG Faults at Zone 1 in the selected microgrid

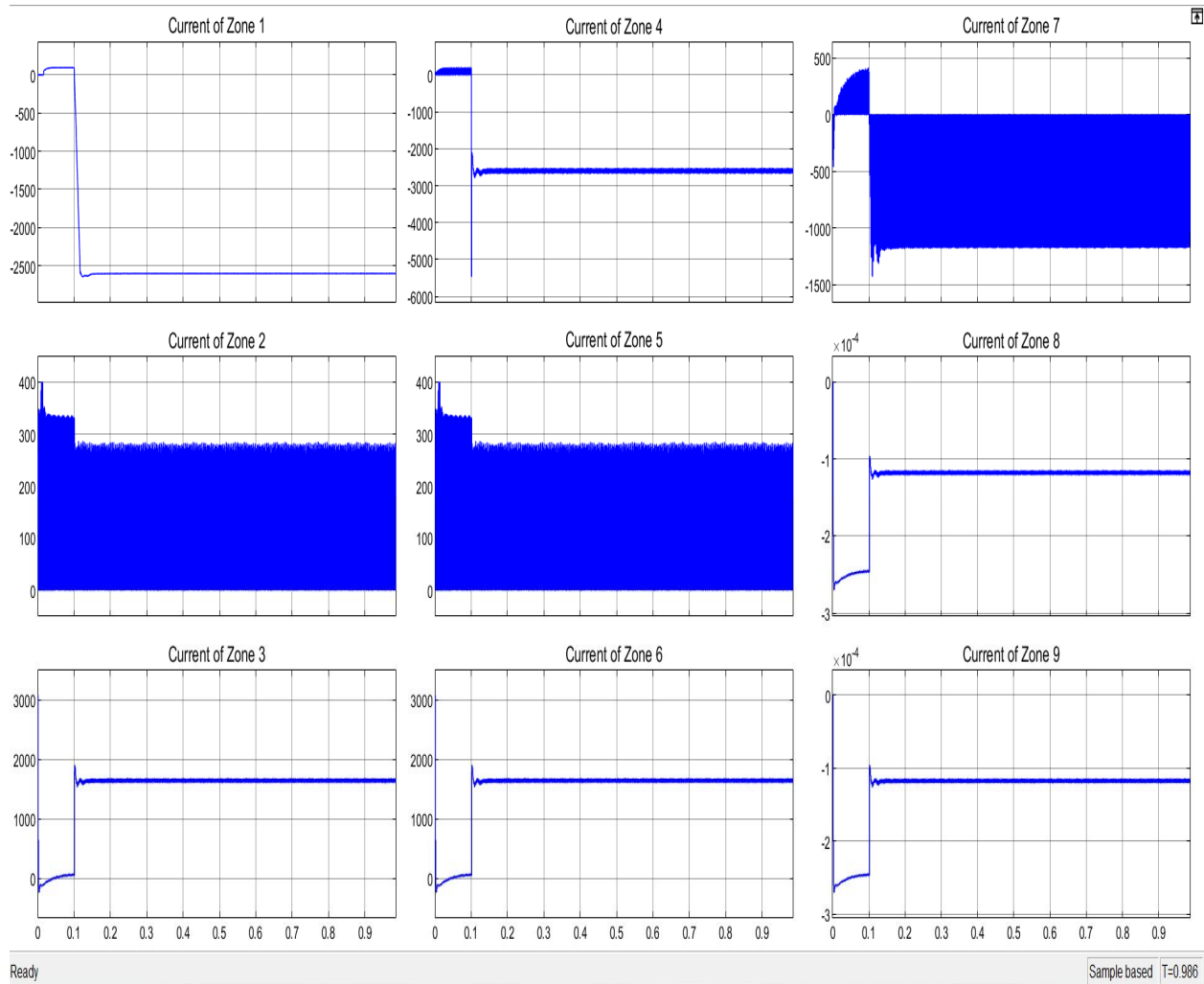


Figure 21

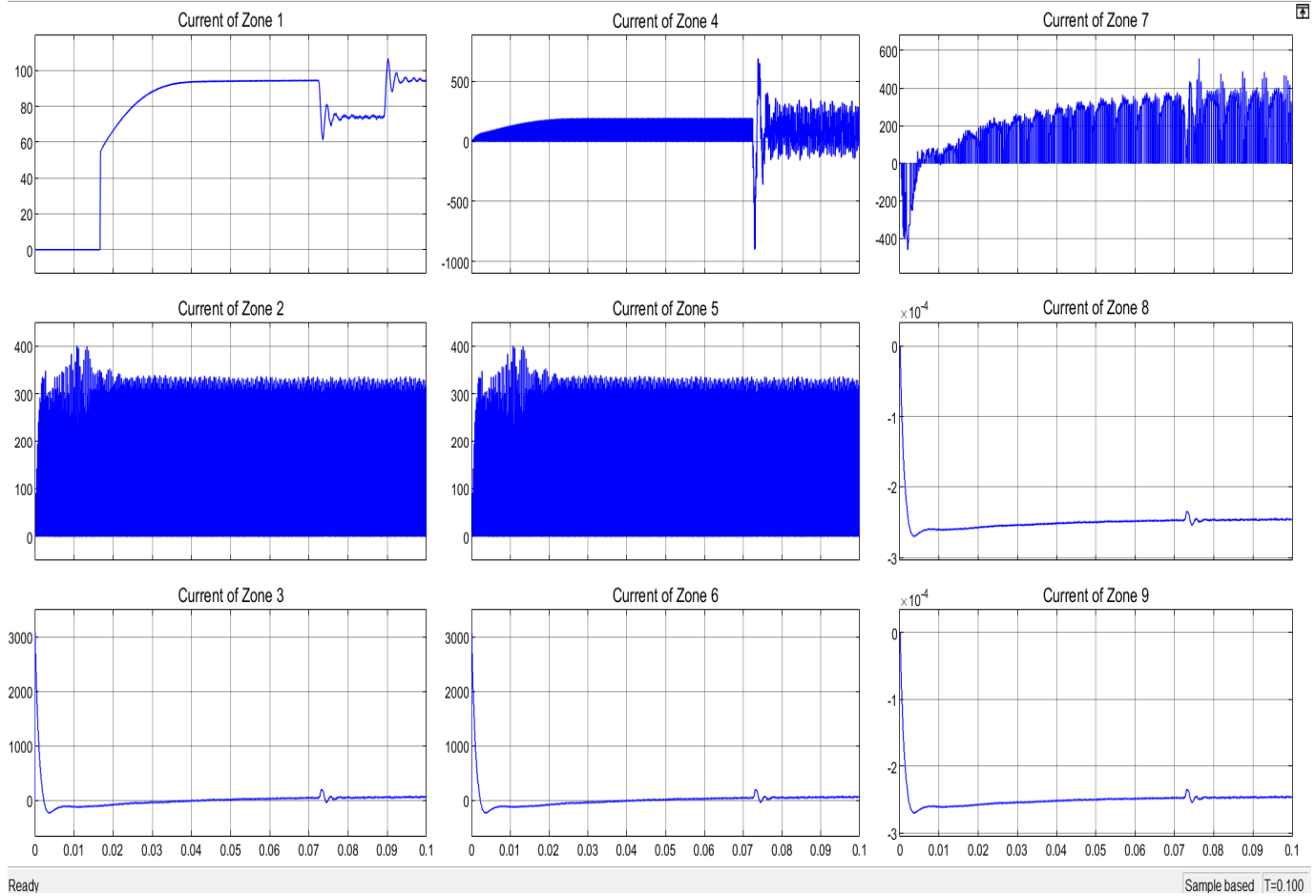


Figure 22

When a pole-to-pole fault is created at Zone 1 as shown in figure 21, the current of zone decreases from a steady state value of approximately 95A to a value of approximately -2600A. The pole-to-pole fault is simulated at a simulation time of 1.00 seconds. However, when a pole to ground fault is created at zone one at a simulation time of 0.07 seconds, Current of all the zones are shown at once (each one explained in earlier section) and the current of zone 1 shows a decrease from the steady value of 95A to around 75A. This decrease is occupied with high harmonics and transients. About 0.02 seconds later, the current increases to the previous steady state value, maintaining the high number of transients.

From Figure 22, It is concluded that a pole-to-pole fault in the studied system has a more severe effect on current than a pole-to-ground fault on the same system.

For protecting the system considered against various types of faults, current change has been monitored at various places with the help of measuring devices available in the mat lab tool box. Fourier transform method has been applied to locate the fault.

D. Algorithm Applied:

In this section of the paper current algorithm for the controller has been discussed which is applied to the microgrid under consideration. Current algorithm works on the principle of finding deviation of the current of the zone with the current of the same section ‘n’ samples ago. In this case value of number of samples taken is 200 per second.

From the current waveforms of various zones shown above, when a fault is created there is a sudden change in the current off that zone and 200 samples back current value has been taken to find the sufficient change in the current of the same zone.

Change in current of a particular zone (ΔI) = Present value of the current - current value 200 samples ago. Following is the algorithm used for fault detection location

$$\Delta I = I_p - I_s(200 \text{ samples back})$$

Current algorithm for fault detection and location for the system under consideration

Start

Measure I

Calculate the value of I 200 previous samples ago

$\Delta I = I - I_{prev}$

If $\Delta I \geq 0.1 * I_{prev}$

Fault detected

F=1

Else

Fault not detected

If F=1

Start fourier transform of current values

Calculate runningmax of magnitude of fourier transform

Runningmax[7] is obtained

Calculate max of all runningmax

If $max == runningmax[0]$

Fault at 1

If $max == runningmax[1]$

Fault at 2

If $max == runningmax[2]$

Fault at 3

If $max == runningmax[3]$

Fault at 4

If $max == runningmax[4]$

Fault at 5

If $max == runningmax[5]$

Fault at 6

If $max == runningmax[6]$

Fault at 7

Repeat until simulation is stopped

Fault is created at 0.051 seconds in zone 4 – breaker of zone 4 shows OFF state Using current algorithm

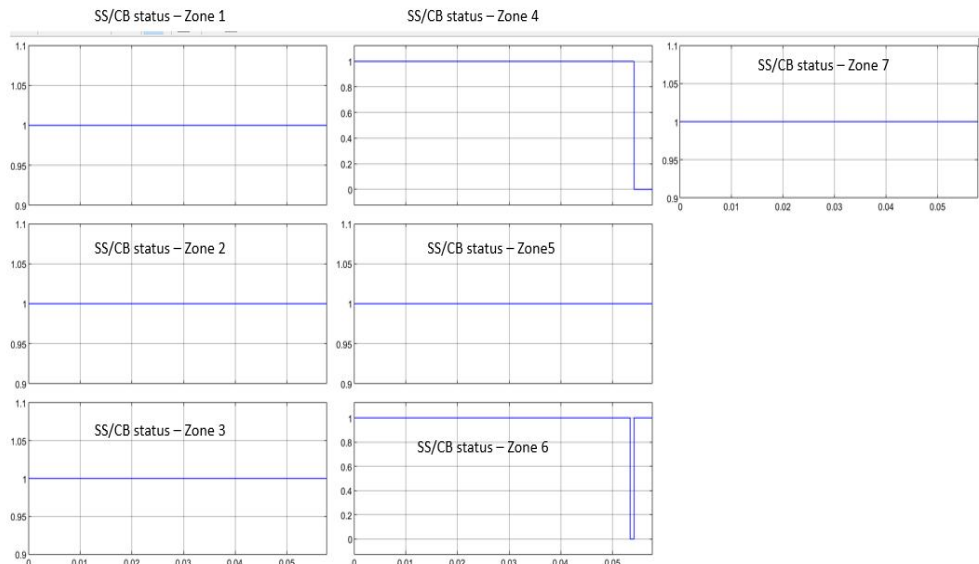


Figure 23

When fault is created at 0.052 seconds the breaker of zone 4 shows OFF state in figure 23 . Fault in 6th zone was also sensed for very short duration, though it did not operate the circuit breaker / smart switch whereas all other CB's or smart switches are closed and showing status as 1.

Current algorithm has been applied to the system under consideration, this algorithm is a memory-based algorithm which required 0.052 seconds wait time to reach steady state before disturbances or faults can affect the system. This algorithm was successful in detecting pole to pole faults and pole to ground faults in the system under consideration. This Current change algorithm made use of dynamically updated values for the operation of smart switches (Isolation switches). It was observed that this method is unable to identify the location of a fault. It takes more than 1 hour to simulate for 0.5 seconds. It took wait time of 0.05 seconds (prerequisite) for the system to reach steady state. So, it is not strongly advised to apply this algorithm for rapidly changing load conditions and irradiation

IV. CONCLUSIONS

Fault Analysis for the system under consideration has been carried out. Current change algorithms has been applied with in the controller for the detection of fault in the microgrid, whereas Fourier transform method has been applied for locating the fault in the microgrid. Current change algorithm is a memory-based algorithm which required some wait time 0.052 seconds wait time to reach steady state before disturbances or faults can affect the system. This algorithm was successful in detecting pole to pole faults and pole to ground faults in the system under consideration. This Current change algorithm made use of dynamically updated values for the operation of smart switches (Isolation switches). It was observed that this method is unable to identify the location of a fault. It takes more than 1 hour to simulate for 0.5 seconds. It took wait time of 0.05 seconds (prerequisite) for the system to reach steady state. So, it is not strongly advised to apply this algorithm for rapidly changing load conditions and irradiation. Machine Learning Based Algorithm can be applied for the protection of microgrid in future as microgrids condition changes at a rate of sub milliseconds.

REFERENCES

- [1] Magdi S.Mahmoud, Mohamed Saif Ur Rahman, Fouad M.A.L.-Sunni, "Review of Microgrid architectures-a system of systems perspective", The Institution of Engineering and Technology (IET) journal, 29th April 2015.
- [2] Robert. H. Lasseter, Paolo Paigi, "Microgrid: A Conceptual Solution" 30th annual IEEE Power Electronics Specialists Conference, Germany, 2004.
- [3] Rahul Anand Kaushik, and N. M. Pindoriya, "A Hybrid AC-DC Microgrid: Opportunities & Key Issues in Implementation", Electrical Engineering, IEEE.
- [4] Xiong Liu, Peng Wang and Poh Chiang Loh, "A Hybrid AC/DC Microgrid and Its Coordination Control", IEEE transactions on smart grid, Vol. 2, No. 2, June, 2011
- [5] Anoop Singh "A market for renewable energy credits in the Indian power sector": Science Direct, Renewable and Sustainable Energy Reviews 13 (2009): 643–652
- [6] Nanfang Yang, Damien Paire, Fei Gao, Abdellatif Miraoui, "Power Management Strategies for Microgrid -A Short Review", IEEE, 2013
- [7] A Hybrid AC-DC Microgrid: Opportunities & Key Issues in Implementation Rahul Anand Kaushik, Student Member, IEEE and N. M. Pindoriya, Member, IEEE Electrical Engineering, Indian Institute of Technology Gandhinagar Ahmedabad, Gujarat, India, Email: rahulanandkaushik@iitgn.ac.in
- [8] Francisc Javoda THE KEY ROLE OF INTELLIGENT ELECTRONIC DEVICES (IED) IN ADVANCED DISTRIBUTION AUTOMATION (ADA) Department of Electrical Apparatus, IREQ (Hydro-Quebec Research Institute), Varennes, PQ, Canada E-MAIL: zavoda.francisc@ireq
- [9] JAFAR MOHAMMADI, (Student Member, IEEE), AND FIROUZ BADRKHANI AJAEI, (Member, IEEE) Electrical and Computer Engineering Department, Western University, London, ON N6A 5B9, Canada" Adaptive Voltage-Based Load Shedding Scheme for the DC Microgrid" current version August 15, 2019
- [10] Sangeeta Modi, P Usha "Mathematical modelling, Simulation and Analysis of Microgrid: A pre-requisite for Devising a Controller" GIS Science Journal, volume 8, Issue 12, December 21, ISSN No: 1869-9391



10.22214/IJRASET



45.98



IMPACT FACTOR:
7.129



IMPACT FACTOR:
7.429



INTERNATIONAL JOURNAL FOR RESEARCH

IN APPLIED SCIENCE & ENGINEERING TECHNOLOGY

Call : 08813907089  (24*7 Support on Whatsapp)